International Journal of Modelling and Simulation, Vol. 27, No. 4, 2007

DEVELOPMENT OF A FULL-BODY BIOMECHANICAL MODEL OF THE GOLF SWING

S.M. Nesbit*

Abstract

This paper presents the development, verification, and application of a full-body biomechanical model of the golf swing. The model consists of a variable full-body computer model of a human interfaced to a flexible model of a golf club, a supporting ground surface, and a ball/club impact force. Data to drive the model are obtained from subject swings recorded using a multi-camera motion analysis system. Model output includes club trajectories, golfer/club interaction forces and torques, joint kinematics, joint loadings, work and power, and club deflections. The model was used to analyse the swings of 84 amateur golfers. The applicable data from these subjects were compared to published data. Experimental and analytical verifications are presented.

Key Words

Biomechanics, modelling, golf, humanoid

1. Introduction

Most biomechanical studies of the golf swing have employed models of varying degrees of sophistication [1–8]. Generally, these models were limited to one or two rigid link (double pendulum) systems and constrained the motion to two dimensions. The double pendulum models were further limited by fixing the pivot point of the upper link. Notable exceptions are Vaughan [7] who analysed the three-dimensional mechanics of a swing using a rigid one-link club model, and Milne and Davis [5] who utilized a two-link planar system with a flexible lower link to study shaft behaviour.

These modelling endeavours have yielded important information on various mechanical quantities of the golf club during the swing. At best however, these models only provided information concerning the cumulative effects or output of the golfer's swing. Inferences to specific body motions and their relative effects on the outcome of the golf swing are difficult and inexact without including the human in golf swing modelling.

* Department of Mechanical Engineering, Lafayette College, Easton, PA, USA; e-mail: nesbits@lafayette.edu
Recommended by Prof. Sundaram Narayanan
(paper no. 205-4599)

One method of obtaining a more complete understanding of the golf swing, and which can be used to identify important swing characteristics for individuals, is the development of a three-dimensional biomechanical model of the golfer [9]. What has limited previous attempts at developing this type of model is the high degree of difficulty in deriving and solving the resulting equations of motion. Fortunately, multi-body analysis software has become available that aides in the development and solution of analytical models for highly complex dynamic systems. This paper presents the development, verification, and application of a full-body biomechanical model of the golf swing which can be used to completely characterize the three-dimensional kinetics and kinematics of the golf club and the joints of the body.

2. Methods and Model

An ambitious research effort was undertaken by the United States Golf Association (USGA) to study all aspects of the golf swing including the biomechanics of the golfer, the interactions between the golfer and his equipment, and the behaviour of the clubs. The specific biomechanical goals were to investigate the mechanics of the golf club during the swing, and more significantly to determine the motions, forces, torques, and energy transfer of the golfer that ultimately produces and influences the motions and behaviours of the club. These goals necessitated a more comprehensive modelling effort which required including the golfer in any biomechanical models.

To help with the development and solution of this highly complex dynamic system the model was derived, analysed, and post-processed with the aid of the commercial software package ADAMS (Mechanical Dynamics, Inc.). An ADAMS model consists of rigid segments connected with flexible elements and/or a variety of joints. Forces and motions can be superimposed on the model. ADAMS derives the differential equations of motion for the model employing methods of Lagrangian dynamics. The resulting equations of motion are integrated using one of several backward differentiation formula (BDF) integrators. The results are output and the model simulated using the ADAMS post-processor. The resulting fully three-dimensional model includes a parametric flexible model of

a golf club, a variable 15-segment model of a golfer, a supporting ground surface, and an impact force (see Fig. 1).

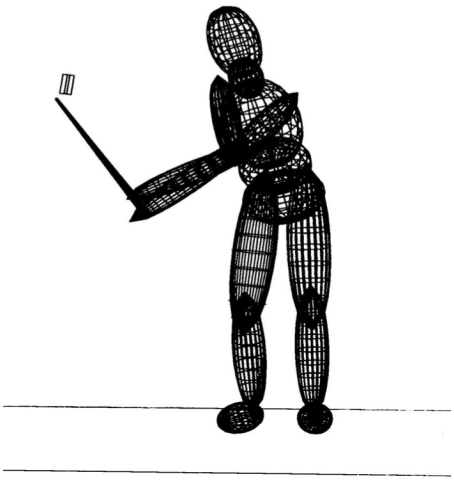

Figure 1. Full-body model of the golf swing.

2.1 Assumptions and Simplifications

The golf swing model consists of the following global elements: a golf club, a humanoid, a ground support surface, and a club/ball impact force. The entire model is treated as rigid with the exceptions of the ground surface, impact force, club shaft, and connections between the hands and the club handle. The joints are modelled as perfect connectors with no damping or relative motion other than the intended joint motion. The joint torques are applied at the joint centres and not resolved into line-of-action muscular forces. The body segments are treated as homogenous solids, however, the mass properties are representative of the general population (see below). The body segment inertia tensors are simplified to include no cross product of inertia terms. A notable generality of the model is the simplified representation of the back, neck, and spine segments and joints. The model divides the entire torso, neck, and spine into three segments and joints (lumbar, thoracic, and neck). A finer division was attempted, however severe marker crowding resulted, and tracking was compromised.

The connections between the hands and the golf club create a potential indeterminate closed-loop configuration. Flexible connectors solved the analytical difficulties (see below); however, it was necessary to assume a load distribution at the hands. An equal load distribution was assumed as no information on load distribution was available. The model does not explicitly define hands. The hands are considered part of the club handle as they have the same kinematic trajectories. The wrist joints attach the end of the forearms to the club handle. The mass properties of both hands are added to the club handle.

A simplification that is especially pertinent to the golf swing is that the model does not account for stored and released muscular strain energy. This simplification is most important at the top of the back swing where there is considerable stored potential strain energy in the body, and static force and torque on the joints due to muscular tension. The next iteration of full-body models should incorporate methods to account for stored and released muscular strain energy and the resulting joint loadings.

2.2 Golfer Model

There are commercial pre-processors that interface with the ADAMS software to create humanoid models (ANDROID (Mechanical Dynamics, Inc.) and LifeMod (Biomechanics Research Group, Inc.)). It is also possible to derive the equations of motion for the humanoid portion of this model using analytical techniques. Which method is preferable depends on the goals of the research. Both methods will be described.

The golfer was modelled as a variable full-body, multilink, three-dimensional humanoid mechanism made up of 15 rigid segments interconnected with joints. The model contains 15 body segments: head, neck, thorax, lumbar, pelvic, upper arm (2), forearm (2), thigh (2), lower leg (2), and foot (2). All segments are defined by their adjacent joints with exceptions of the neck (C1–C8), thorax (T1–T12), and lumbar (L1–L5 and S1–S5) which are defined by the associated vertebrae. The individual body segments are ellipsoid in shape (see Fig. 2) with the segment size, mass, and inertia properties determined from gender, age, and overall body height and weight, or from local segment measurements using the GeBod database accessible through the ADAMS software, or from one of the many references concerning body segment mass properties [10].

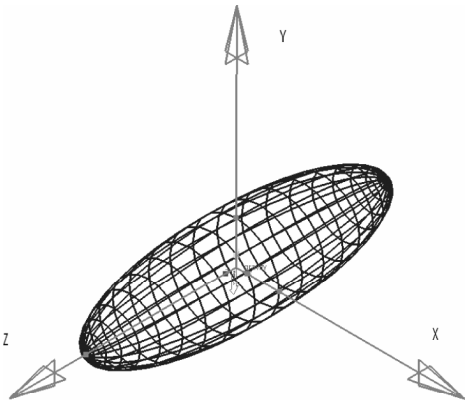

Figure 2. Body model segment shape showing principal coordinate system.

The body segment reference coordinate systems, established when the subject is standing in the standard anatomical position, place the Z-axis pointing downward with the exception of the feet which point forward parallel to the long axis of the foot segment. The X-axis points outward from the body and the Y-axis completing a right-handed coordinate system. Joint motions, forces, and torques are of the distal body segment coordinate system relative to the proximal body segment coordinate system. The angular quantities are specified according to the relative body (Euler angle) 1-2-3 Bryant angle convention where alpha motion (α) is about the X-axis, beta motion (β) is about the Y-axis, and gamma motion (γ) is about the Z-axis [11].

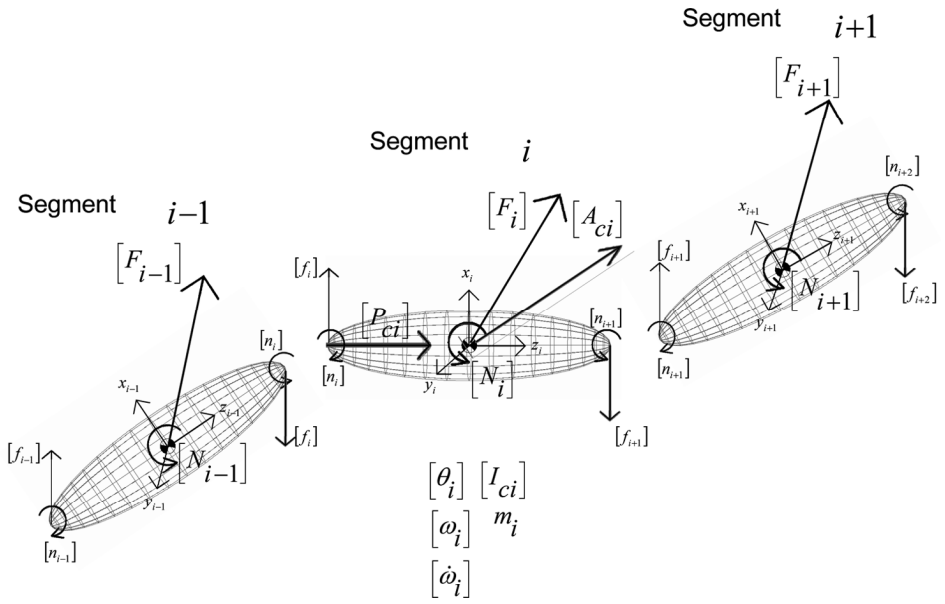

Figure 3. Free-body diagrams of body segments in serial chain.

The model consists of 15 joints: ankles (2), knees (2), hips (2), lumbar, thoracic, neck, shoulders (2), elbows (2), and wrists (2). All joints are spherical yielding a maximum of three relative angular degrees-of-freedom (DOFs) with the exceptions of the knees and elbows which are modelled as one DOF revolute joints. The motions superimposed upon the spherical joints are specified by all three Bryant angles and their time-dependent derivatives (angular velocities and accelerations). The revolute joint motions correspond to the beta Bryant angle and its derivatives only.

The equations of motion for the humanoid model can be derived using any standard method of three-dimensional rigid-body dynamic analysis. The method that is most easily applied to this model is the iterative Newton–Euler dynamic formulation. This method is often used for serial chain robot manipulator arms [12]. The iterative nature of this method refers to the sequential development of the equations of motion for a serial chain of rigid bodies which is the configuration of open-loop robot manipulators and the humanoid portion of this model. Referring to Fig. 3 which shows free-body diagrams of three adjacent body segments $i-1$ (proximal), i, and $i+1$ (distal), the force and moment balance on body segment i yield Newton's equation (1) and Euler's equation (2):

$$ {}^{i}f_i = {}^{i}_{i+1}R^{i+1}f_{i+1} + {}^{i}F_i \tag{1} $$

$$ {}^{i}n_i = {}^{i}N_i + {}^{i}_{i+1}R^{i+1}n_{i+1} + {}^{i}Pc_i \times + {}^{i}F_i + {}^{i}P_{i+1} \times {}^{i}_{i+1}R^{i+1}f_{i+1} \tag{2} $$

where the inertial forces and moments are:

$$ {}^{i+1}F_{i+1} = m_{i+1}{}^{i+1}Ac_{i+1} \tag{3} $$

$$ {}^{i+1}N_{i+1} = {}^{i+1}Ic_{i+1}{}^{i+1}\dot{\omega}_{i+1} + {}^{i+1}\omega_{i+1} \times {}^{i+1}Ic_{i+1}{}^{i+1}\omega_{i+1} \tag{4} $$

and the mass centre linear acceleration is:

$$ {}^{i+1}Ac_{i+1} = {}^{i+1}\dot{\omega}_{i+1} \times {}^{i+1}Pc_{i+1} + {}^{i+1}\omega_{i+1} \times ({}^{i+1}\omega_{i+1} \times {}^{i+1}Pc_{i+1}) + {}^{i+1}A_{i+1} \tag{5} $$

where:

$$ {}^{i+1}A_{i+1} = {}^{i+1}_{i}R({}^{i}\dot{\omega}_i \times {}^{i}P_{i+1} + {}^{i}\omega_i \times ({}^{i}\omega_i \times {}^{i}P_{i+1})) + {}^{i}A_i \tag{6} $$

where for all the variables, the subscript refers to the body segment, the superscript to the body segment frame of reference and:

R is the 3×3 transformation matrix

f is the 3×1 vector of link interaction forces

F is the 3×1 vector of inertia forces at the link mass centre

n is the 3×1 vector of link interaction torques

N is the 3×1 vector of inertia moments

Pc is the 3×1 position vector of the link mass centre

P is the 3×1 position vector of the link

A is the 3×1 linear acceleration vector

Ac is the 3×1 linear mass centre acceleration vector

m is the link mass

Ic is the 3×3 inertia tensor about the link mass centre

ω is the 3×1 angular velocity vector

$\dot{\omega}$ is the 3×1 angular acceleration vector

The R matrices map quantities from one frame of reference to another. The form of the transform depends on the type of joint and the angle representation. The element values of the transform matrix are a function of the joint angles. A complete discussion of transformation matrices can be found in [12]. The form of the R matrix for a spherical joint and a body 1-2-3 Euler angle representation is the following:

R_{11}	R_{12}	R_{13}
R_{21}	R_{22}	R_{23}
R_{31}	R_{32}	R_{33}

where:

$$R_{11} = \cos\alpha\cos\beta \tag{7}$$

$$R_{12} = \cos\alpha\sin\beta\sin\gamma - \sin\alpha\cos\gamma \tag{8}$$

$$R_{13} = \cos\alpha\sin\beta\cos\gamma - \sin\alpha\sin\gamma \tag{9}$$

$$R_{21} = \sin\alpha\cos\beta \tag{10}$$

$$R_{22} = \sin\alpha\sin\beta\sin\gamma - \cos\alpha\cos\gamma \tag{11}$$

$$R_{23} = -\sin\alpha\cos\beta \tag{12}$$

$$R_{31} = -\cos\alpha\sin\beta\cos\gamma - \sin\beta\sin\gamma \tag{13}$$

$$R_{32} = \cos\alpha\sin\beta\sin\gamma - \sin\alpha\cos\gamma \tag{14}$$

$$R_{33} = \cos\alpha\cos\beta \tag{15}$$

The form and elements of the transform matrix for a revolute joint are the same with the alpha and gamma angles set to zero.

Equations (1) through (6), the transformation matrix, and the free-body diagrams of Fig. 3 can all be easily extrapolated to the humanoid model because of the serial arrangement of the rigid links and joints in configuring the arms, legs, torso, and head and neck. The indicial form of (1) through (6) facilitates the programming of these expressions to either solve them directly as a numerical computational algorithm or to derive the symbolic equations of motion [12]. This indicial notation also obscures the number, form, and tremendous complexity of these equations which require computer assistance to derive and solve.

The pelvic body segment is designated as segment 0. Global accelerations of the body are applied to the mass centre of this segment. Outward iterations from this segment compute the inertial forces and torques acting on each segment ((3) and (4)) from the mass centre accelerations (5). These calculations depend on joint angles, velocities, and accelerations which are obtained from subject swing data and the subsequent calculations of Appendices A and B. Once the ends of each serial chain is reached (arms, legs, head/neck, etc.), the iterations reverse and work inward to determine joint forces and torques from (1) and (2). Adding a club to the analytical model is accomplished by creating a club model as described in the following section and analysing it separately. This analysis solves for the driving forces and torques at the club handle. These forces and torques are distributed and superimposed at the ends of the arms where the club would attach (avoiding the closed-loop configuration). Thus, once the inertia tensor, masses, and mass centre vector are specified for each body segment, the R matrices computed for each joint from the joint angles ((7) through (15)), the joint velocities and accelerations determined by numerical differentiation, and the club forces and torques determined for the separate club model, the Newton–Euler equations can be applied directly to compute the joint torques and interaction forces for any imposed motion [12]. This inverse dynamic analysis results in equations that are linear in form thus quite solvable, and yield the time histories of the joint forces and torques that cause a pre-specified motion, i.e., the subject's recorded swing.

2.3 Club Model

The golf club was modelled as a flexible stepped shaft joined to a rigid club head. The shaft was made up of 15 rigid sub-segments each with representative mass and inertia properties. The sub-segments were connected by massless three-dimensional beam elements with the appropriate flexibility and damping characteristics. The mass and flexibility properties for the shaft sub-segments were calculated using standard analytical methods for a hollow cylinder. Global shaft damping was determined experimentally by fixing the grip end of a club in a cantilever manner, deflecting the club head, and measuring the rate of amplitude decay. This value was assumed to apply to all shaft sub-segments. The rigid club head segment with hosel contains the representative mass, CG location, and 3×3 inertia tensor which were determined using solid modelling techniques [13], experimental methods [14], or published data. Analytical methods for deriving and solving the equations of motion for a golf club with a three-dimensional flexible shaft are presented in [15].

The club and the golfer models were interconnected with spherical-type joints placed at the ends of the lower arms and attached to the grip point of the shaft to simulate the motions of the wrists. The three angular DOFs of both joints were driven kinematically while the three linear DOFs were designated as flexible for both joints. This designation avoided a closed-loop (indeterminate) configuration while still yielding the resultant interaction forces and torques between the golfer and the club. The flexibility constants were adjusted until an approximately equal linear force was supported by both wrists.

2.4 Swing Data and Joint Motions

Data to kinematically drive the joints of the golfer model were obtained from subject golf swings. A multi-camera motion analysis system tracked passive–reflective markers (13 and 19 mm in diameter) that were strategically placed on the golfer and the club. There were 23 markers placed on the golfer and 3 on the club. On the golfer the markers were placed at the wrists, forearms, elbows, shoulders, cervical and lumbar vertebra, head, hips, knees, mid-lower leg, ankles, and feet. All markers were located relative to bony landmarks for subject-to-subject consistency, and securely attached with two-sided tape (skin) or Velcro (clothing). Markers were attached directly to the skin wherever possible. The subjects wore snug-fitting clothing (tank-top and bicycle-style shorts), a baseball hat (head marker), and shoes of their choice. Marker/joint offsets were measured, and virtual joint centre markers were located from these

data using features provided by the data collection software. The three markers on the club were arranged in a rigid triad that was attached to the shaft just below the handgrip.

The three-dimensional marker paths were recorded at 180 Hz (see Fig. 4) then smoothed and processed to yield global body 1-2-3 angular motions of each body segment and the club. The global angular motions were transformed into local relative joint motions by comparing the motions of adjacent body segments. This process is described in Appendix A. The joint relative angular velocities and accelerations were determined directly from the joint angles using methods of numerical differentiation that are described in Appendix B. The relative angular motions were used to kinematically drive the joints of the golfer model.

Figure 4. Stick figure model of recorded golf swing.

2.5 Impact Model

A spring–damper impact function was included to model the ball-club head collision at impact. The impact force is calculated from the expression:

$$F = KX^e - CV \tag{16}$$

where X is the impact deformation, V is the impact deformation velocity, K is the spring stiffness, e is the stiffening exponent, and C is the damping factor. The values for K ($K = 912{,}975\,\mathrm{N/m}$) and e ($e = 1.5265$) were obtained from static compression tests performed on a variety of golf balls [16]. The damping factor C was set to 5% as no experimental or analytical data were available. This value was selected as it reflects the under-damped impact phenomena, and it results in a rapid removal of impact energy without noticeably increasing the impact force. The impact force (Fig. 5) calculated from (16) gave results consistent with published impact forces [17, 18]. More sophisticated impact models may be found in [19].

2.6 Ground Surface Model

A ground surface model was added to support the golfer. A standard linear spring–damper system was used to represent the contact between the feet and the ground, and frictional forces provided traction. The initial contact parameters were obtained from [20] and were adjusted at solution time to prevent over-stiffening the model. The golfer model was balanced by kinematically driving the angular DOFs of the lower torso segment (hips) relative to the global coordinate system. To avoid over-constraining the model, the linear DOFs were set free.

Individual force plates were used to measure the vertical reaction forces between the golfer's feet and the ground. The data provided some kinetic verification of the model because ground reaction forces are one of the outputs of the model (see Section 3). The data were also used to cause the model to keep both feet on the ground. A kinematically driven model is infinitely stiff, therefore, small joint angle errors can cause one of the feet to leave the ground surface. To solve this problem, the beta motion (up and down) of one of the ankle joints was dynamically driven to give the model compliance. A torque control function (17) that incorporated the force plate data was applied to the beta motion of the ankle joint to force the foot down is given by:

$$T_{Beta} = \sum Ci(F_{MEAS} - F_{CALC})^{Pi} + T_{WEIGHT} \tag{17}$$

where T_{Beta} is the applied torque, Ci and Pi are the function constants, F_{MEAS} and F_{CALC} are the measured and calculated ground reaction forces, respectively, and

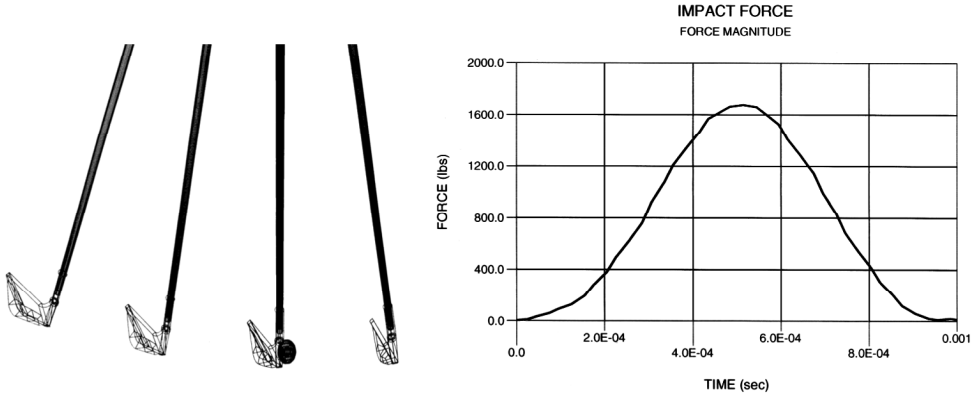

Figure 5. Simulated impact for iron club head.

T_{WEIGHT} is the torque in the ankle joint imposed by the weight of the golfer on that foot. The function constants are adjusted through trial solutions. Once an acceptable set of torque control function constants was found, the solution was iterated until the individual ground reaction forces from the analysis matched the data from each force plate.

2.7 Work and Power

Traditional kinetic analyses of the golfer have focused on determining the forces and torques generated during the downswing [9]. However, this information provides insight to instantaneous accelerations, not overall changes in velocity thus yielding a snapshot image of the swing dynamics. An energy analysis has the following advantages: only the forces/torques that change the velocity of the club are taken into account, i.e., forces/torques that do no work are ignored; the cumulative effects of forces/torques applied over a distance are determinable which introduces factors such as range of motion, timing, and sustainability of forces/torques; the collective effect of various body motions can be summarized by looking at the energy transferred to the club and the resulting club velocity [21].

The work and power expressions were developed from the general analytical equation for the work on a rigid body in three-dimensional motion:

$$Work_{Golfer} = \int_{t_2}^{t_1} \left(\sum \vec{F}_i \cdot \vec{V}_i + \vec{\omega}_i \cdot \sum \vec{N}_i \right) dt \qquad (18)$$

where $\vec{F}_i$ is the external force vectors, $\vec{V}_i$ is the linear velocity vector, $\vec{\omega}_i$ is the angular velocity vector, and $\vec{N}_i$ is the external moment vector. The spherical joints behave kinematically as three orthogonal revolute joints. A higher-order pair joint being replaced by a configuration of lower pair joints is a standard analytical tool of mechanism analysis [22]. The body 1-2-3 Euler angle representation specifies that the axes of motion of the revolute joints line up with, and move sequentially with respect to the X, Y, and Z axes of the proximal segment. From this configuration it can be seen that numerically the work of the joints can be determined by summing each separate angular movement over time as:

$$Work_{Joint} = \sum_{0}^{n} T_\alpha(\alpha_{t+\Delta t} - \alpha_t) + \sum_{0}^{n} T_\beta(\beta_{t+\Delta t} - \beta_t) + \sum_{0}^{n} T_\gamma(\gamma_{t+\Delta t} - \gamma_t) \qquad (19)$$

where n is the number of numerical time steps, T_α, T_β, and T_γ are the torque components, t is the time, and Δt is the time interval. The work of the joints during the downswing for four right-handed subjects is shown in Fig. 6 and clearly illustrates the importance of the back and hips in swinging the golf club. Joint power can be determined by substituting the angular velocities for the joint angles in (19).

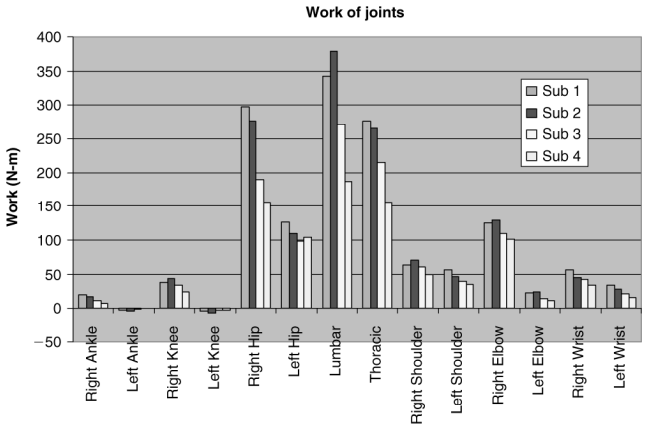

Figure 6. Work of joints during the downswing.

2.8 Solution and Model Output

A summary of the steps necessary to create each modelling element, collect subject swing data, and solve the model is presented in the following flow chart. The flow chart assumes a pre-processor is used to create the humanoid portion of the model (Fig. 7).

The primary component of the model, the humanoid is rigid and kinematically driven yielding simultaneous linear equations which results in a closed-form solution. However, the other model components are the ground surface, flexible golf club shaft, hand/club connection, and the impact force, introduced non-linearities and time-dependent dynamic responses into the system. Thus, the entirety of the model represents a forward dynamics or simulation problem requiring numerical integration to solve. The resulting dynamic equations of motion were solved using a Wielenga Stiff Integrator (Mechanical Dynamics Inc.). Solution of the model yielded a simulation of the swing (Fig. 1), the three-dimensional club trajectories (Fig. 8), club kinematics, golfer/club interaction forces and torques, club work and power, club deflections (Table 2), joint kinematic and kinetic quantities (Fig. 10), joint work and power (Fig. 6), ground reaction forces (Fig. 9), and impact forces (Fig. 5). Other examples of model output are given in Section 3.

3. Model Verification and Application

Verification of the model was done in four phases. First, the simulated swing and joint motions of the model were compared to the motion analysis data and joint motion calculations for kinematic verification. Second, several test simulations were run and compared to closed-form solutions. Third, the ground reaction forces predicted by the model were compared to force plate data. And fourth, several subjects were analysed using the model and the resulting output compared to available published data.

3.1 Kinematic Verification

The kinematic verification compared the simulated swing and joint motions of the model with the motion analysis data and joint motion calculations. The joint angles for the

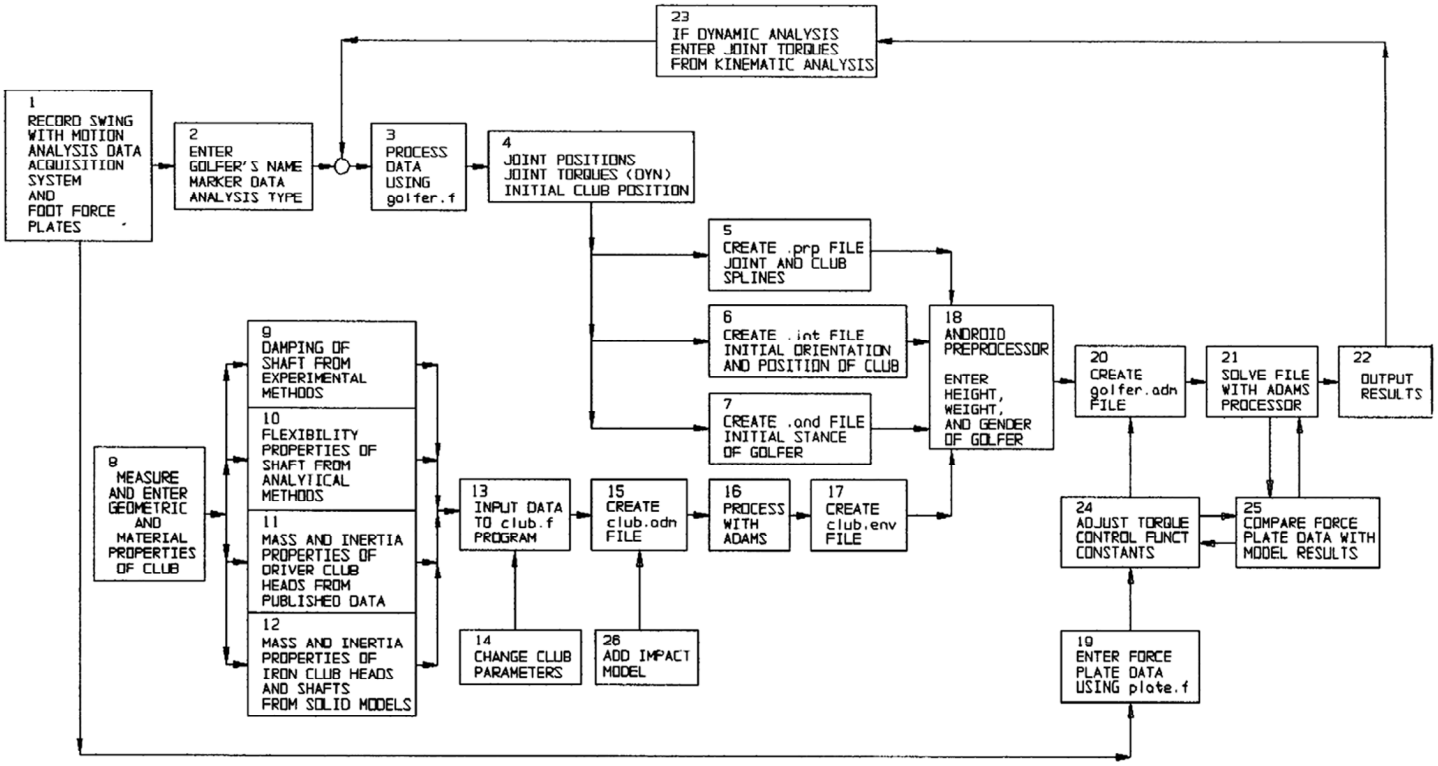

Figure 7. Model creation flow chart.

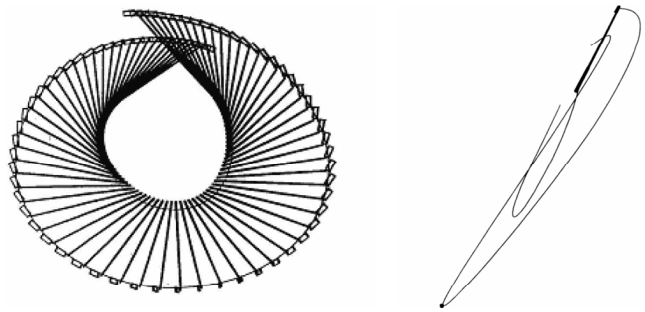

Figure 8. Front and side views of superimposed simulation of subject swing.

model were calculated from the marker data using the analytical methods described in Appendix A. The joint angular velocities and accelerations were subsequently determined from the analytical methods described in Appendix B. These kinematic quantities were used to drive the joints of the model. The model simulations exactly reproduced the subjects' motions in terms of joint angles, velocities, and accelerations providing kinematic verification of the model.

3.2 Test Simulations

To verify the joint forces and torques predicted by the model, several static and inverse dynamic test cases were applied to the model and compared to analytically predicted results. The static analyses consisted of posing the humanoid model in a variety of stationary positions (such as the arms straight out to the side) and having the model solve for the static torques and forces in the joints to support the segments against gravitational loads. The model results and analytically determined results were identical. Next, harmonic motions were applied to individual segments (inverse dynamic simulation) and the model determined joint torques were compared to analytically predicted joint torques. Both methods gave identical results.

A forward dynamic analysis verification was attempted. Using the results of a kinematically driven simulation of a golf swing, the model predicted joint torques were subsequently used to redrive the joints to see if the motion of the original simulated swing was recreated. It succeeded in cases where only one DOF of the joints was torque driven while the other two were kinematically driven. In cases where all three DOFs were torque driven, the resulting motions were unpredictable, and the simulation failed.

3.3 Experimental Verification

The one kinetic output of the model that could be directly and accurately measured was ground reaction forces. The vertical reaction forces measured by the force plates and predicted by the model were each summed for both feet and compared (Fig. 9). Force plate data compared well with model calculated vertical ground reaction forces. While this one corroboration of predicted load data from the model is certainly not complete, coupled with the other verifications, it does increase confidence in both the validity of the model, and its ability to predict internal loads.

3.4 Published Data

Previous efforts to analyse the golf swing by means of computer modelling relied upon models of the club or two-

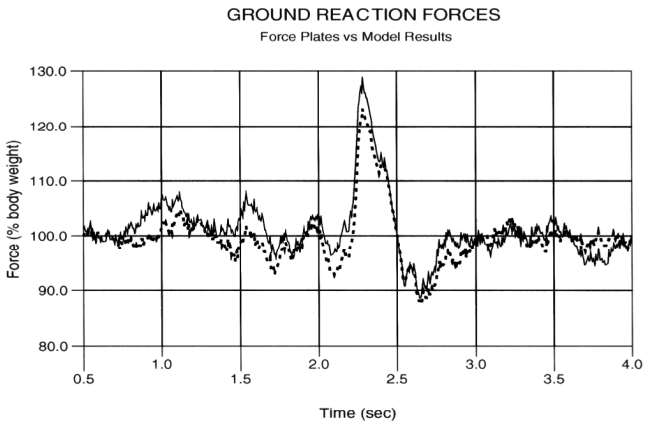

Figure 9. Force plate data (dots) versus model predicted ground reaction forces (line).

link models; thus, the existing data that is relevant to this model are limited to the kinematic and kinetic quantities of the club. A review of the literature revealed that there are data for the following quantities: club head velocity, grip velocity, magnitude of the linear interaction force, the alpha component of angular velocity, the three components of the interaction torques, club shaft deflections, club energy, and club power.

To be able to compare the data from this model to published results, the reference system for the club was changed slightly and is described as follows. The reference coordinate system, established when the subject addresses the ball, places the X-axis (alpha) perpendicular to the club shaft and aligned with the bottom edge of the club face as viewed down the club shaft, the Z-axis (gamma) pointing down the club shaft, and the Y-axis (beta) completing a right-handed coordinate system. The alpha component coincides with the swing angular motion, the beta component is a measure of the pitch motion of the club relative to the swing, and the gamma component is the roll angular motion about the long axis of the shaft.

A total of 84 male (right-handed) amateur golfers of various skill levels, experience, age, height, weight, and competitive rounds played per year have had their swing recorded then analysed using this computer model. A summary of the subject data is given in Table 1. All subjects used the same driver club for the data presented here.

Informed consent for the following procedure was obtained from all of the subjects. Each subject had reflective markers placed upon his body. After practicing for several minutes to acclimate to the markers and surroundings, the subjects were asked to execute a series of swings which included striking a golf ball. A swing from each subject was self-selected then analysed. Table 2 presents the statistical summary of the entirety of the kinematic and kinetic quantities of the club for all the subjects including the average, median, standard deviation, and range. The quantities are reported for the downswing to impact portion of the swing. The (M) refers to maximum values and (I) to values at impact. The time relative to impact is given in parentheses. These data form the basis for comparisons to published data.

Table 3 gives the relevant published data from the literature. In all cases, the reported values are for one subject only with the exception of [2] which reported some values for four subjects. The models used were all two-link, two-dimensional, rigid models with the exception of Vaughan [7] who used a one-link rigid three-dimensional model, and Milne and Davis [5] who utilized a two-link planar system with a flexible lower link.

The magnitude of the grip velocity agrees well with [7]; however, there was not the significant reduction in hand speed prior to impact as reported and which is discussed in [23]. The maximum club head velocity values and velocity profiles agree with all reference values. The alpha component of the angular velocity is slightly lower than that reported in [2] which is most likely due to the faster club head velocity of their subject (52.6 m/s versus 46.4 m/s). The magnitude of the linear force at the grip and the shape of these curves agree well with the published data. Alpha torque magnitudes are near the average of the extreme values reported in [1, 7]. However, the torque profiles are quite different. The beta torque values are about half the magnitude reported in [7], and these curve profiles are also quite different. The gamma torque magnitudes and profiles obtained are considerably different than those reported in [7]. The club deflection magnitudes and profiles generally agree with those obtained in [5]. The work of the club agrees with that reported in [2] and is higher than that reported in [24]. No work profiles were given. Maximum club power agrees well with published data. No power profiles were given.

Differences in Table 2 values versus the published data of Table 3 can be attributed to differences in individual subjects, the clubs used, the modelling and analysis methodologies, testing circumstances, etc. It is not possible to isolate which of these factors either individually or combined, account for differences in values and profiles from this model compared to reported values. Even so,

Table 1
Subject Data

	Age	Height (cm)	Weight (kg)	Handicap	Experience (years)	Rounds per Year
Average	31.6	182.3	83.9	5.8	15.8	58.9
Median	28.0	182.9	81.8	6.0	12.0	45.0
Standard deviation	10.6	7.8	8.8	6.0	11.3	56.6
Range	18–56	168.0–193.0	70.5–109.1	0–20	5–35	20–200

Table 2
Swing Analysis Data (Time Relative to Impact)

Data	Units	Average	Median	Standard Deviation	Range
Club Head Vel (M)	m/s	46.37 (−0.002)	47.25 (0.000)	4.98 (0.005)	39–52
Club Head Vel (I)	m/s	46.25	46.00	2.87	43–50
Grip Vel (M)	m/s	8.125 (−0.003)	8 (0)	0.25 (0.030)	7.8–8.5
Grip Vel (I)	m/s	7.75	8	0.50	7.1–8.0
Alpha Vel (M)	Deg/s	1,756.25 (−0.020)	1,762.5 (−0.030)	123.11 (0.008)	1,600–1,910
Alpha Vel (I)	Deg/s	1,737.5	1,775	94.65	1,600–1,900
Beta Vel (M)	Deg/s	68.75 (−0.176)	70 (−0.197)	57.209 (0.134)	30–125
Beta Vel (I)	Deg/s	−145	−165	212.17	100–(−375)
Gamma Vel (M)	Deg/s	−231.25 (−0.200)	−237.5 (−0.200)	24.75 (0.000)	−200–(−250)
Gamma Vel (I)	Deg/s	−925	−925	301.39	−600–(−125)
Alpha Accel (M)	Deg/s^2	10,312.5 (−0.060)	10,125 (−0.062)	2,248.8 (0.015)	8,000–13,000
Alpha Accel (I)	Deg/s^2	−1,587.5	−2,550	3,949.34	−4,100–3,750
Beta Accel (M)	Deg/s^2	4,650 (−0.019)	5,300 (−0.015)	2,594.22 (0.012)	1,000–7,000
Beta Accel (I)	Deg/s^2	2,450	1,500	2,282.54	1,000–5,800
Gamma Accel (M)	Deg/s^2	1,650 (−0.050)	−450 (−0.050)	5,661.9 (0.057)	−2,500–10,000
Gamma Accel (I)	Deg/s^2	2,500	3,000	7,000	−6,000–10,000
Linear Force (M)	N	395 (−0.015)	395 (−0.015)	84.16 (0.006)	300–490
Linear Force (I)	N	397.5	400	87.70	300–490
Club Lin Accel (M)	m/s^2	1,441.3 (−0.008)	1,437 (−0.010)	304.0 (0.005)	1,090–1,800
Club Lin Accel (I)	m/s^2	1,475	1,500	312.2	1,100–1,800
Grip Lin Accel (M)	m/s^2	170 (−0.010)	165 (−0.005)	24.5 (0.014)	150–201
Grip Lin Accel (I)	m/s^2	163.7	162.5	16.0	150–175
Alpha Torque (M)	N-m	30.88 (−0.074)	30.75 (−0.087)	9.187 (0.038)	22–40
Alpha Torque (I)	N-m	4.25	9	17.15	−20–5
Beta Torque (M)	N-m	10.78 (−0.088)	11.75 (−0.088)	2.62 (0.0322)	7–12.6
Beta Torque (I)	N-m	−2.625	−3.125	4.264	−6.25–2
Gamma Torque (M)	N-m	1.375 (−0.043)	−0.2 (−0.030)	3.25 (0.043)	−0.3–6.25
Gamma Torque (I)	N-m	0.0625	−0.125	0.5089	−0.3–0.8
Club Defl (M)	m	0.1088 (−0.035)	0.105 (−0.045)	0.02594 (0.024)	0.085–0.14
Club Defl (I)	m	0.06125	0.0675	0.04007	0.085–0.01
Total Work (M)	N-m	291.75 (−0.012)	288.5 (−0.010)	49.13 (0.015)	235–355
Total Work (I)	N-m	287.25	285	50.29	28–351
Total Power (M)	N-m/s	2,727.5 (−0.048)	2,657.5 (−0.053)	927.92 (0.017)	1,720–3,875
Total Power (I)	N-m/s	237.5	250	587.89	−450–900

there appears to be sufficient agreement among the various reported values and the comparable data from this model to yield confidence in the kinematic and kinetic values predicted for the club.

It is clear that limiting models to two-dimensional motion and fixing the upper pivot point for two-link models are overly restrictive. For example, Fig. 8 shows a non-circular path of the hands which could not be recreated with a fixed upper pivot point. This non-circular path has been shown to be an important component in generating club head velocity [25]. In addition, the side view of the swing shows two planes, one containing the path of the hands and the other the path of the club head. These different planes indicate that considerable pitch (beta angle) motion of the club occurs. The data for the beta quantities in Table 2 support this finding. Two-dimensional models remove the beta motion completely. The substantial club deflections reported in Table 2 validate the inclusion of a flexible model of the shaft of the club.

The model also outputs the joint kinematic and kinetic quantities including work and power. An example for one subject is given in Fig. 10 which plots the time history of the angular velocity and displacement of the twisting motion of the lumbar joint, and the three components of the lumbar joint torque.

Table 3
Relevant Published Data

Data Type	Units	Reference Values
Club Head Vel	m/s	49.5 [8], 40.5 [23], 42.6 [3], 42.7 [1], 51.0 [7], 52.6 [2], 43.5 [24]
Grip Velocity	m/s	(9.5 max and 8.0 at impact) [7]
Alpha Velocity	Deg/s	2,074 [2]
Max Linear Force	N	476 [8], 400 [1], 364 [7], (266–364) [2]
Alpha Torque	N-m	21.8 [1], 52.0 [7]
Beta Torque	N-m	23 [7]
Gamma Torque	N-m	(7.0 max and 2.5 at impact) [7]
Shaft Deflection	m	0.087 [6]
Club Work	N-m	(266–311) [2], 220.8 [24]
Club Power	N-m/s	3,000 [23], 2,750 [1], (2,530–3,640) [2]

4. Discussions and Conclusions

This paper presents the development, verification, and application of a full-body model of a golf swing created for the purpose of furthering the understanding of golf swing biomechanics. This model represents an evolution over previous golf swing models through the inclusion of the full-body golfer model, the flexible stepped shaft club model, the ground surface model, and impact model. This modelling effort consciously avoided applying the simplifying assumptions that limited previous modelling attempts. While there are pre-processors available for creating the humanoid portion of the model, the iterative Newton–Euler dynamic formulation method developed for serial chain robot manipulators proved to be an effective analytical method for deriving the equations of motion without the aid of a pre-processor. Methods for determining joint angles from motion analysis marker path data were presented using the body 1-2-3 Euler angle representation. Numerical differentiation schemes were presented as alternative methods to calculate joint velocities and accelerations directly from joint positions. The ADAMS software was used to create the club and ground models, combine the elements of the model, derive and solve the equations of motion, and post-process the results.

The use of the ADAMS software and associated pre-processors greatly aided in the development of the model. However, there is a trade-off between the understanding and insight gained through deriving the model by analytical means, and the ability to create more complex and representative models through the use of the software. For example, if one is only interested in the model output quantities, then the use of the software alone is satisfactory. If there is a need to perform in-depth investigation of the terms in the equations of motion and their form, then the iterative Newton–Euler dynamic formulation method is preferred.

Various methods of model verification were presented including comparisons to motion analysis data, joint motion calculations, test simulations, force plate data, and available published data. It is certain from the verifications that the model can be kinematically controlled to simulate a subject's swing in terms of matching the joint positions, velocities, and accelerations yielding a global recreation of the recorded motion. The agreement of the force plate data with model predicted ground reaction forces coupled with agreement of the club kinematic and kinetic quantities with independent comparable data gives confidence in the model's ability to predict the output of the golf swing, i.e., how the golfer interacts with the ground and the club, and the actions of the golfer in swinging the club. Verification of internal joint forces and torques was more difficult, especially as no published data were available for comparison. The test simulations would lend support that at the very least the model predicted internal forces and torques are correct based on the limitations of the model. These simulations together with the other verifications yield some degree of confidence in how well the predicted joint forces and torques represent the actual loads in the subjects' joints.

The model is a valuable tool for investigating and describing the golf swing through the capacity to simulate

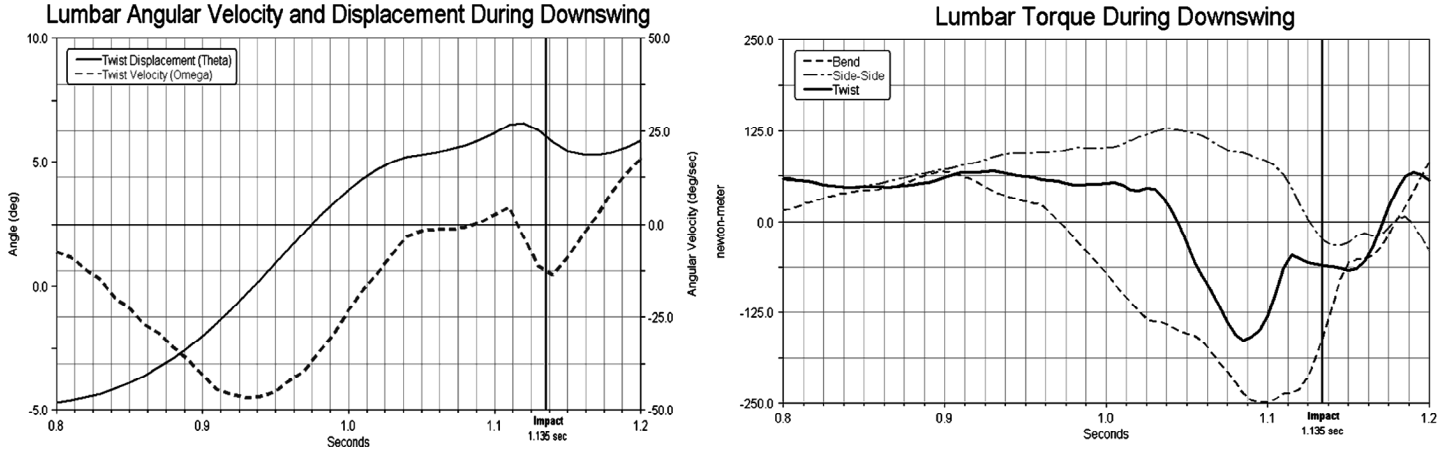

Figure 10. Joint kinematic and kinetic data predicted by the model.

and completely characterize the three-dimensional kinematics and kinetics of the club and golfer's joints. In addition to the data and figures provided in this paper, the model has been used successfully to analyse the swings of many subjects [26], study the wrists [25], perform a work and power analysis [21], quantify club aerodynamic effects [27], and investigate club head inertia tensor effects [28].

Acknowledgements

Funding for this project was provided by grants from the United States Golf Association and the National Science Foundation.

References

[1] D.R. Budney & D.G. Bellow, Kinetic analysis of a golf swing, *Research Quarterly*, *50*(2), 1979, 171–179.

[2] D.R. Budney & D.G. Bellow, On the swing mechanics of a matched set of golf clubs, *Research Quarterly for Exercise and Sport*, *53*(3), 1982, 185–192.

[3] T. Jorgensen, On the dynamics of the swing of a golf club, *American Journal of Physics*, *38*(5), 1970, 644–651.

[4] M.A. Lampsa, Maximizing distance of the golf drive: An optimal control study, *Journal of Dynamic Systems, Measurement, and Control, Transactions ASME 97 (Series G)*, December, 1975, 362–367.

[5] R.D. Milne & J.P. Davis, The role of the shaft in the golf swing, *Journal of Biomechanics*, *25*(9), 1992, 975–983.

[6] R.J. Neal & B.D. Wilson, 3D kinematics and kinetics of the golf swing, *International Journal of Sport Biomechanics*, *1*(3), 1985, 221–232.

[7] C.L. Vaughan, A three-dimensional analysis of the forces and torques applied by a golfer during the downswing, *Biomechanics VII-B*, Warsaw (Poland: University Park Press, 1981), 325–331.

[8] D. Williams, The dynamics of the golf swing, *Quarterly Journal of Mechanics and Applied Mathematics*, *20*, 1967, 247–255.

[9] C.J. Dillman & G.W. Lange, How has biomechanics contributed to the understanding of the golf swing? in A.J. Cochran & M.R. Farrally (Eds.), *Proc. 1994 World Scientific Congress of Golf*, St. Andrews, Scotland, 1994, 1–13.

[10] D.A. Winter, *Biomechanics and motor control of human movement* (New York: John Wiley & Sons, Inc., 1990).

[11] T.R. Kane, P.W. Likins, & D.A. Levinson, *Spacecraft dynamics* (New York: McGraw-Hill Co., 1983).

[12] J.J. Craig, *Introduction to robotics: Mechanics and control* (Reading, MA: Addison-Wesley Publishing Co., 1986).

[13] K.A. Oglesby, J.S. Cole, & S.M. Nesbit, Parametric ANSYS model of golf clubs, *Proc. 1992 ANSYS Technical Conference*, Pittsburgh, PA, 1992, 1107–1112.

[14] S.H. Johnson, Experimental determination of inertia ellipsoids, in A.J. Cochran & M.R. Farrally (Eds.), *Proc. 1994 World Scientific Congress of Golf*, St. Andrews, Scotland, 1994, 290–295.

[15] A.M. Brylawski, An investigation of three-dimensional deformation of a golf club during downswing, in A.J. Cochran & M.R. Farrally (Eds.), *Proc. 1994 World Scientific Congress of Golf*, St. Andrews, Scotland, 1994, 265–270.

[16] S.H. Johnson, Experimental determination of the static mechanical properties of golf balls, *USGA Technical Report* (United States Golf Association, Far Hills, NJ, 1995).

[17] W. Gobush, Impact force measurements on golf balls, in A.J. Cochran & M.R. Farrally (Eds.), *Proc. 1990 World Scientific Congress of Golf*, St. Andrews, Scotland, 1990, 219–223.

[18] S. Ujihashi, Measurement of the dynamic characteristics of golf balls and identification of the mechanical properties, in A.J. Cochran & M.R. Farrally (Eds.), *Proc. 1994 World Scientific Congress of Golf*, St. Andrews, Scotland, 1994, 302–308.

[19] B.B. Lieberman & S.H. Johnson, An analytical model for ball-barrier impart, Part 1 and Part 2, in A.J. Cochran & M.R. Farrally, *Proc. 1994 World Scientific Congress of Golf*, St. Andrews, Scotland, 1994, 309–319.

[20] S. Scott & D. Winter, Biomechanical model of the human foot: Kinematics and kinetics during the stance phase of walking, *Journal of Biomechanics*, *26*(1), 1993, 1091–1104.

[21] S.M. Nesbit, Work and power analysis of the golf swing, *Proc. 2003 ASME Annual Bioengineering Conference*, Miami, FL, 2003, 199.

[22] R.L. Norton, *Design of machinery* (New York: McGraw-Hill Publishing, Inc., 1992).

[23] A. Cochran & J. Stobbs, *The search for the perfect swing* (New York: J.P. Lippincott Co., 1969).

[24] T. Jorgensen, *The physics of the golf swing* (New York: API Press, 1994).

[25] S.M. Nesbit, 3D mechanics of the wrist during the golf swing, *Proc. American College of Sports Medicine Annual Conference*, San Francisco, CA, 2003.

[26] S.M. Nesbit, Three-dimensional kinematic and kinetic study of the golf swing, *USGA Technical Report*, Research and Test Center, United States Golf Association, Far Hills, NJ, 1998.

[27] M. Baumgartner, A.J. Smits, & S.M. Nesbit, Effect of aerodynamic modifications to golf clubs. *USGA Technical Report*, Research and Test Center, United States Golf Association, Far Hills, NJ, 1997.

[28] S.M. Nesbit, T.A. Hartzell, J.C. Nalevanko, R.M. Starr *et al.*, A discussion of iron golf club head inertia tensors and their effects on the golfer, *Journal of Applied Biomechanics*, *12*(4), 1996, 449–469.

[29] R.K. Dean & S.M. Nesbit, Evaluation of finite difference schemes for the solution of the inverse velocity and acceleration problem for robot manipulators, in Birendra Prasad (Ed.), *Proc. Third Int. Conf. on CAD/CAM, Robotics, and Factories of the Future*, Southfield, MI, 1988, 210–216.

Appendix A: Determination of Joint Angles

Local coordinate systems were defined for each body segment (and the club) from groups of three adjacent marker locations. Generally, markers were placed at the distal and the proximal ends of each segment, and are represented as markers $i+1$ and i, respectively. In addition, a third non-collinear marker is placed between markers i and $i+1$, and is designated marker $i+2$. Taken together, the three markers form a plane from which the local coordinate systems are established. The local Z-axis is coincident to the long axis of the segment and is determined from the following vector difference:

$$\begin{matrix} Z_x \\ Z_y \\ Z_z \end{matrix} = \begin{matrix} X_{i+1} \\ Y_{i+1} \\ Z_{i+1} \end{matrix} - \begin{matrix} X_i \\ Y_i \\ Z_i \end{matrix} = \{\hat{Z}\} \tag{1A}$$

An intermediate vector Q is determined from markers i and $i+2$:

$$\begin{matrix} Q_x \\ Q_y \\ Q_z \end{matrix} = \begin{matrix} X_{i+2} \\ Y_{i+2} \\ Z_{i+2} \end{matrix} - \begin{matrix} X_i \\ Y_i \\ Z_i \end{matrix} = \{\hat{Q}\} \tag{2A}$$

Using cross products, the local X and Y axes can be determined as follows:

$$\{\hat{Z}\} \times \{\hat{Q}\} = \{\hat{Y}\} = \begin{matrix} Y_x \\ Y_y \\ Y_z \end{matrix} \tag{3A}$$

$$\{\hat{Y}\} \times \{\hat{Z}\} = \{\hat{X}\} = \begin{matrix} X_x \\ X_y \\ X_z \end{matrix} \quad (4A)$$

The local coordinate system is then represented in matrix form as follows:

X_x	Y_x	Z_x
X_y	Y_y	Z_y
X_z	Y_z	Z_z

where the first column X_x, X_y, X_z is the X-axis unit vector components, the second column is the Y-axis unit vector components, and the third column is the Z-axis unit vector components. This process is repeated for all body segments and the club. All of the terms in the above matrix are known.

The ANDROID model is driven kinematically by specifying the relative body 1-2-3 Euler angles (Bryant angles alpha (α), beta (β), and gamma (γ)) for each joint. The Bryant angle transformation matrix is as follows:

R_{11}	R_{12}	R_{13}
R_{21}	R_{22}	R_{23}
R_{31}	R_{32}	R_{33}

where:

$$R_{11} = \cos\beta\cos\gamma \quad (5A)$$
$$R_{12} = -\cos\beta\sin\gamma \quad (6A)$$
$$R_{13} = \sin\beta \quad (7A)$$
$$R_{21} = \sin\alpha\sin\beta\cos\gamma - \cos\alpha\sin\gamma \quad (8A)$$
$$R_{22} = -\sin\alpha\sin\beta\sin\gamma - \cos\alpha\cos\gamma \quad (9A)$$
$$R_{23} = -\sin\alpha\cos\beta \quad (10A)$$
$$R_{31} = -\cos\alpha\sin\beta\cos\gamma - \sin\alpha\sin\gamma \quad (11A)$$
$$R_{32} = \cos\alpha\sin\beta\sin\gamma - \sin\alpha\cos\gamma \quad (12A)$$
$$R_{33} = \cos\alpha\cos\beta \quad (13A)$$

The local coordinate system matrix and the Bryant angle transformation matrix are set equal to each other for each segment. Thus, the left-hand sides of (5A) through (13A) are known. From these equations, the global Bryant angles are extracted. For example, solving for the angle α, note the following:

$$Z_y = R_{23} = -\sin\alpha\cos\beta \quad (14A)$$
$$Z_z = R_{33} = \cos\alpha\cos\beta \quad (15A)$$

Dividing (14A) by (15A) yields the formula for α:

$$\alpha = \tan^{-1}(Z_y/Z_z) \quad (16A)$$

Using a similar procedure, the expressions for β and γ are found:

$$\beta = \tan^{-1}((Z_x/(Z_y^2 + Z_z^2))^{1/2}) \quad (17a)$$
$$\gamma = \tan^{-1}(-Y_x/X_x) \quad (18a)$$

Thus, (16A), (17A), and (18A) yield the global Bryant angles for each body segment and the club. Relative angles of the distal segment with respect to the proximal segment are needed to drive the joints of the model. Determination of the relative Bryant angles is done the following way. The relationship between the Bryant matrices of adjacent segments is given by:

$$^G_D R = {}^G_P R\, {}^P_D R \quad (19A)$$

where G is the ground (global reference system), D is the distal segment, and P is the proximal segment. The relative Bryant angles are contained inside the $^P_D R$ matrix. To isolate this matrix, both sides of (19A) are multiplied by the inverse of the $^G_P R$ matrix yielding:

$$[{}^G_P R]^{-1}\, {}^G_D R = {}^P_D R \quad (20A)$$

The global Bryant angles are substituted into the $^G_D R$ and $^G_P R$ matrices yielding all known elements of the $^P_D R$ matrix. The relative Bryant angles are then extracted from the $^P_D R$ matrix in a manner similar to that used for the global Bryant angles. Application of (20A) to the digitized motion analysis data yields tabular three-dimensional relative motions for all the joints of the model including the wrists which drive the club. Cubic splines are used to create continuous functions from the tabular data to kinematically drive each joint.

Appendix B: Determination of Joint Velocities and Accelerations

The determination of joint angular velocities and accelerations can be determined from marker paths using closed-form analytical methods for multi-link robotic arms as described in [12]. An alternative method is to use numerical differentiation. For smooth trajectories, the use of the appropriate differentiation scheme can yield accurate results [29]. The author has found that the following schemes were the most accurate for this application. For the calculation of joint relative angular velocities, the following forward, backward, and central difference equations (of error order δt^2, δt^2, and δt^4, respectively) were used:

$$\{\omega\}_i = \frac{-\{\theta\}_{i+2} + 4\{\theta\}_{i+1} - 3\{\theta\}_i}{2\delta t} \quad \text{for } i = 0,\ 1 \quad (1B)$$

$$\{\omega\}_i = \frac{3\{\theta\}_i - 4\{\theta\}_{i-1} + \{\theta\}_{i-2}}{2\delta t} \quad \text{for } i = n-1,\ n \quad (2B)$$

$$\{\omega\}_i = \frac{-\{\theta\}_{i+2} + 8\{\theta\}_{i+1} - 8\{\theta\}_{i-1} + \{\theta\}_{i-2}}{12\delta t} \quad \text{for } i = 2 \text{ to } n-2 \quad (3B)$$

For the calculation of joint relative angular accelerations, the following forward, backward, and central difference equations (of error order δt, δt, and δt^2, respectively,

which calculated the acceleration directly from the joint positions) were used:

$$\{\dot{\omega}\}_i = \frac{\{\theta\}_{i+2} - 2\{\theta\}_{i+1} + \{\theta\}_i}{\delta t^2} \quad \text{for } i = 0 \tag{4B}$$

$$\{\dot{\omega}\}_i = \frac{\{\theta\}_i - \{\theta\}_{i-1} + \{\theta\}_{i-2}}{\delta t^2} \quad \text{for } i = n \tag{5B}$$

$$\{\dot{\omega}\}_i = \frac{\{\theta\}_{i+1} - 2\{\theta\}_i + \{\theta\}_{i-1}}{\delta t^2} \quad \text{for } i = 1 \text{ to } n-1 \tag{6B}$$

Biography

Steven Nesbit is an Associate Professor and Head of the Mechanical Engineering Department at Lafayette College, Easton, PA. He received his B.S., M.S., and Ph.D. degrees in Mechanical Engineering from West Virginia University. Prior to joining the faculty at Lafayette College, he was a design engineer for Pratt-Whitney Aircraft. His research interests are in the fields of biomechanics, mechanisms, and engineering education. Professor Nesbit is a registered Professional Engineer in the Commonwealth of Pennsylvania.